The Study of the Lifting Arm System and Its Experimental Model for Integrated Offshore Platform Decommissioning

Changjiang Li*, Wensheng Xiao, Teng Wang, Xianglin Qu, Quan Li and Lianghuan Fan

College of Mechanical and Electronic Engineering, China University of Petroleum (East China), Qingdao, Shandong, China 266580

* Corresponding Author Email: lichangjiang@s.upc.edu.cn

Abstract. With the further exploitation of offshore oil and gas resources, there are more and more offshore oil and gas fields cannot meet the production capacity requirements. Therefore, the decommissioning of the offshore facilities becomes extremely urgent. In this article, the study of the lifting arm system for the integrated ultra-large offshore platform decommissioning, which is a part of the "Special Vessels and Equipment" program of the Ministry of Industry and Information Technology, is studied and its experimental model is built. First, the prototype structure of the lifting arm system is studied, and a statics simulation analysis to the lifting arm is performed to determine that its structural strength meets the requirements for decommissioning operations. The scale ratio of the experimental model is deduced using the principle of similitude, appropriate materials are selected, and statics analysis of the lifting arm model is performed to ensure that it meets the strength requirements. This is a pioneering research in China and lays a good foundation for subsequent model experiments of decommissioning operations and the development of physical equipment.

Keywords: integrated decommissioning, lifting arm system, experimental model, and finite element analysis.

1. Introduction

The double-ship integrated offshore platform decommissioning equipment is a brand new set of offshore equipment. The lifting arm and the supporting structure are special and there is little design experience about it. Meanwhile, the optimizing of the design of the lifting arm and the supporting structure is critical in the design of the integrated offshore platform decommissioning equipment. Its design directly determines the realization of the technical target and operational safety of the entire decommissioning equipment. Since the integrated ultra-large offshore platform decommissioning equipment cannot be experimented with physical vessels, it is urgently required to perform model experimental research to provide a reliable and accurate research platform for the subsequent development of equipment.

Related researches by other researchers provides a certain reference for the study in this paper. Regarding to the study of model experiments, Wang et al. [1] brought up a general structural dynamics model that predicts the natural frequencies of a folding wing with simplified geometry but with an arbitrary number of wing segments. Yuan[2] et al. analyzed the application and development of modal model experiments and the ability to effectively convert it into visualization tools based on linearity/superposition linearity of structural dynamics. Chi Shichun[3] et al. verified the gravity similarity law by conducting structural model experiments on organic glass materials. Liu Zeyu[4] proposed a similarity criterion suitable for heave compensation systems based on the principle of similitude, and developed the scaled test prototype on the premise of satisfying the principle of similitude. DanHong Li[5] designed a model experiment based on the principle of similitude, conducted multiple experimental verifications, and finally designed an knuckle-joint press that can adapt to parameter changes. H. Q. Lan[6] et al. establish a cable-stayed bridge model experiment based on the principle of similitude, and verified the system reliability through the comparison of experiments and numerical simulations. Ling Li[7] et al. designed an experimental model of a heavy-loaded beam based on the principle of similitude, and verified the correctness of the established experimental model through comparing the modal parameters by combining finite element and experimental modal analysis techniques. Wang Zhenyu[8] et al. established a scaled experimental model of friction materials based on the principle of similitude, and conducted comparative experiments between the actual object and the model. Song Rengqun[9] applied the principle of similitude and found the similarity requirements and conversion relationships of model experiments by dimensional analysis and equation analysis.

In this article, the prototype of the lifting arm is first analyzed. Then, the scale ratio of the model experiment is deducted based on the principle of similitude and the experimental model is designed. Then, finite element analysis is performed to the prototype and experimental model of the lifting arm to verify if the structural strength can meet the design requirements, which lays a foundation for the future researches.

2. The Design of the Lifting Arm and Its Experimental Model

2.1. Description of the Integrated Offshore Platform Decommissioning Solution

To adapt to the development trend of international marine engineering, especially in response to the demand for decommissioning of ultra-large offshore platforms, it is planned to design and develop a lifting equipment with a capacity of not less than 20,000 tons for joint offshore lifting operations. After a comprehensive analysis of the technical characteristics of various offshore platform decommissioning solutions at home and abroad, the integrated ultra-large offshore platform decommissioning solution is proposed as shown in Fig. 1.

Fig. 1 Integrated Ultra-large Offshore Platform Decommissioning Solution

This decommissioning solution consists of three semi-submersible barges equipped with DP3 positioning system, in which two of them are for decommissioning operations and the other one for transportation. During operations, the two semi-submersible barges will totally provide a lifting force of over 32,000 tons and the other barge will ship the decommissioned platform away.

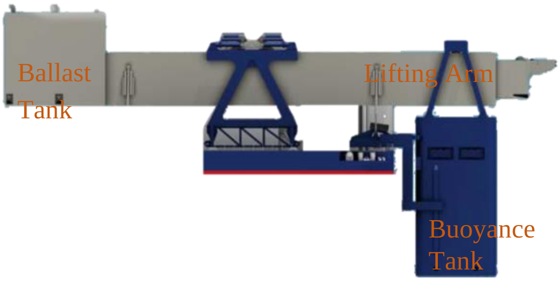

Fig. 2 Illustration of Semi-submersible Barge **Fig 3** Simplified Structure of Lifting Arm

The lifting arms are connected flexibly internally. Each lifting arm can work individually, which ensures a flexible installation and decommissioning of the topside, supports and subsea structures of the drilling and exploitation platforms. The lifting arms and the hulls are connected tightly with a stable internal structure. The lifting principle of the solution is as illustrated in Fig. 4. The buoyancy tanks of the lifting arms provide a moment upward (as marked by the orange arrows), the ballast tanks provide a moment downward (as marked by the yellow arrows) and the two semi-submersible barges serve as the supporting points (as marked by the white arrows) to generate a lifting force upward (as marked by the green arrows) at the end of the lifting arm, so as to lift the platform to be decommissioned.

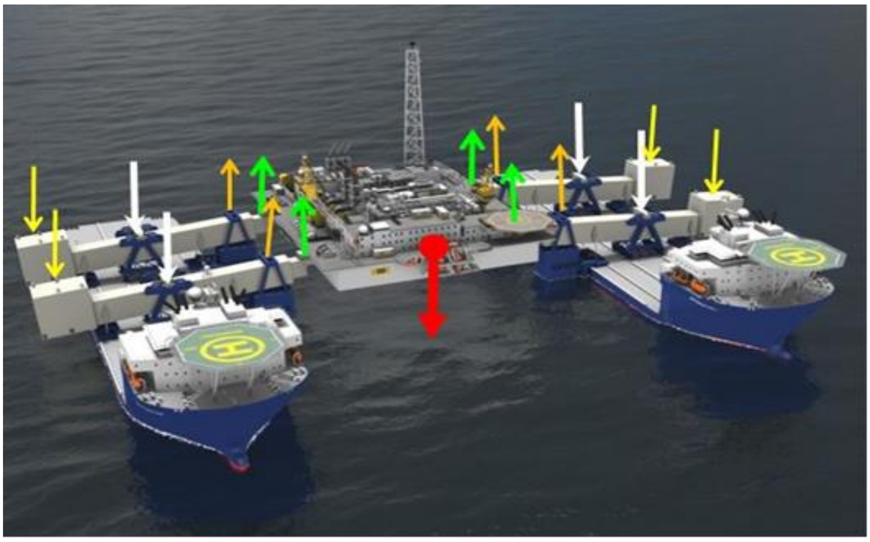

Fig. 4 Illustration of the Lifting Principle

The working procedures of integrated offshore platform decommissioning solution is as follows:

Weigh the topside. Determine the quantity and capacity of lifting arms to be used based on the weight and specify the center of gravity to guarantee the balance during operations.

Install the lifting fixture.

Pump in the ballast water. Determine the amount of ballast water needed to form a lifting force sufficient to float the target platform based on the weighing results and buoyancy calculation.

Float. Discharge ballast water to form buoyancy that can offset gravity, and lift the target platform assembly.

Transfer the lifted platform to the third transport barge. The first two semi-submersible barges will cooperate to lift the topside or supports of the target platform as a whole, and then transfer it to the third semi-submersible barge simultaneously based on the precise positioning of the DP3 positioning system, and transport it to the shore.

Unload the platform from the barge for dismantling.

2.2. The Design of Lifting Arm

2.2.1 The Structure Design of the Lifting Arm

During the joint lifting process, the lifting arm and its supporting structure have to bear the load from the self-weight of the object being lifted, the environment load from wind, current and waves, the relative motion load of the barges, and the inertial load generated by the buoyancy tank and the ballast tank, etc. The various loads coupled with each other will be significantly different under different operating conditions. Therefore, the lifting arm is designed with ribbed slabs and reinforcing ribs inside to ensure that the strength of the lifting arm and its supporting structure meets the requirements.

The lifting arm is divided into two parts: the main arm structure, which is 73 meters in length, including the ballast tank, main arm and slide rails of the telescopic arm, which is as shown in Figure 5; the other structure is the telescopic arm which moves laterally. The telescopic arm is 36 meters in length and its structure is as shown in Figure 6.

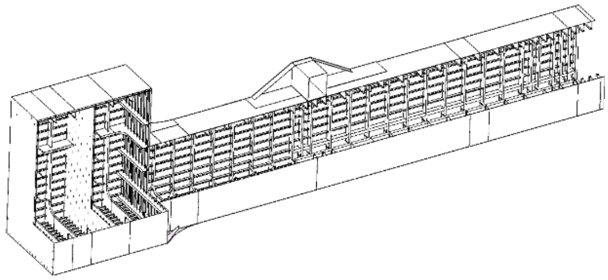

Fig. 5 Three-dimensional Model of Main Arm Structure

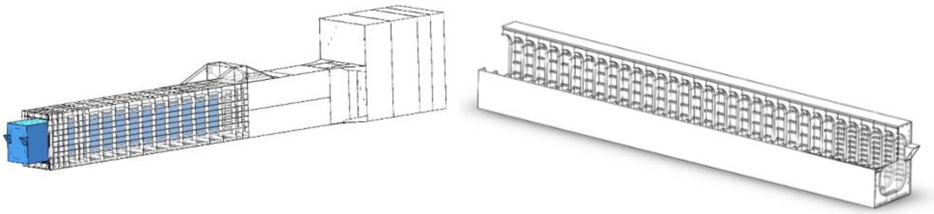

Fig. 6 Three-dimensional Model of Telescopic Arm

2.2.2 Material Characteristics of the Lifting Arm

The material characteristics of the lifting arm is as shown in Table 1.

Table 1 Material Characteristic Parameters of Lifting Arm

Young's Modulus	Poisson's Ratio	Density	Limit State	ULS	Yield Strength
200000 N/mm²	0.3	7850 kg/m³	Structural Steel	1.15	355Mpa

2.3. The Design of Lifting Arm Experimental Model

2.3.1 The Structure Design of the Experimental Model

In order to accurately reflect the effectiveness of the experiment, the scale is strictly in accordance with the ratio between the actual size to the experimental model. The geometric similitude ratio of the integrated decommissioning experimental system is determined as $C_L = 50$ with the limit of the testing area and testing equipment, which is also in line with the reference value of the commonly used geometric similarity constants of beam-plate structures.

According to the determined similitude criteria for integrated decommissioning equipment, an experimental model of the lift arm is established and corresponding structures are simplified, so as to restore the structural characteristics of the lifting arm to meet the experiment requirements and simplify the lifting arm structure to facilitate the manufacturing of the experimental model at the same time.

The main purpose of this model experiment is to verify the reliability of collaborative control and the critical sea conditions for operations. The structural strength of the lifting arm only needs to meet the strength requirements. Therefore, the internal ribbed slabs and reinforcing ribs are removed, and the telescopic arm is bonded with the main arm into a whole, and the lifting arm is disassembled into a plate-like structure according to the molding characteristics of the organic glass plate. The three-dimensional model of the lifting arm is as shown in Figure 7.

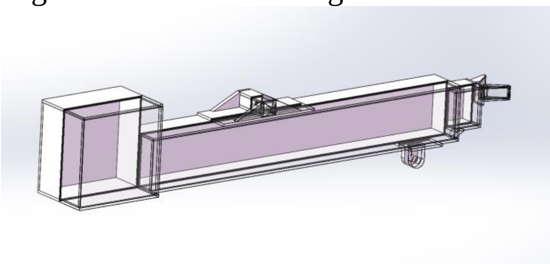

Fig. 7 Three-dimensional Model of Experimental Model

With the principle of keeping the lifting arm experimental model consistent with the prototype, the length, width and height adopt the unified scaling ratio of $C_L = 50$. After scaling, the total length of the lifting arm experimental model is 1660mm, the width is 216mm, and the height is 280mm. The lifting arm is hollow inside, and the various organic glass plates are connected with rivets and reinforcing plate structures.

2.3.2 Material Characteristics of the Experimental Model

The material characteristics of the experiment model is as shown in Table 2.

Table 2. Material Characteristic Parameters of Experimental Model

Tensile Strength (MPa)	Compressive Strength (MPa)	Bending Strength (MPa)	Elasticity Modulus (MPa)	Poisson's ratio	Specific Weight (10^4 N/m^3)
75.8	135.9	110.2	3000	0.35	1.2

3. Finite Element Analysis

3.1. Finite Element Model

3.1.1 The Finite Element Model of the Lifting Arm

The finite element model of the lifting arm is established in the software based on the three-dimensional model of the lifting arm and meshed as shown in Figure 8.

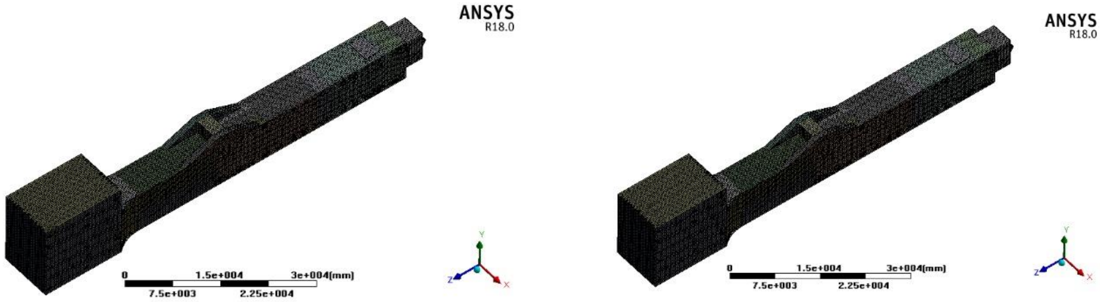

Fig. 8 Finite Element Model of the Lifting Arm

3.1.2 The Finite Element Model of the Experimental Model

The finite element model of the experimental model is established and meshed as shown in Figure 9.

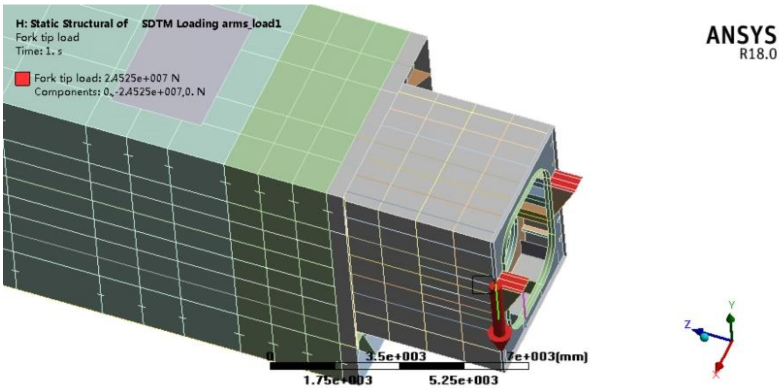

Fig. 9 Finite Element Model of Experimental Model

3.2. Loading Mode

3.2.1 The Loading Mode of the Lifting Arm

Load boundary conditions: The total self-weight of the structure is 1,120.7t, and the applied acceleration of gravity is 9.806m/s. There are three loads added to the lifting arm, namely the ballast tank load, the buoyancy tank load and the load on the fork structure. The specific forces are as shown in Figure 10.

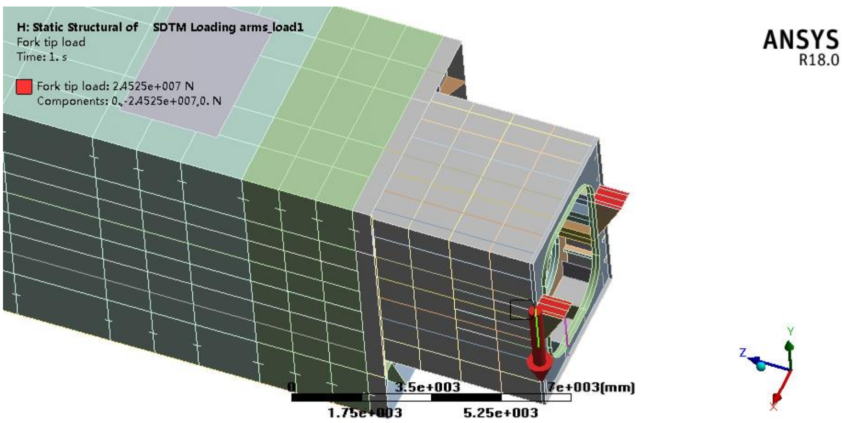

The F_{Fork} is the gravity of the object to be lifted and F_{Fork}=24525kN in the analysis.

Fig. 10 The Force Diagram of the Lifting Arm

The load on the fork structure: The load on where the fork contacts with the lifting fixture is present in the form of static force as shown in Figure 11.

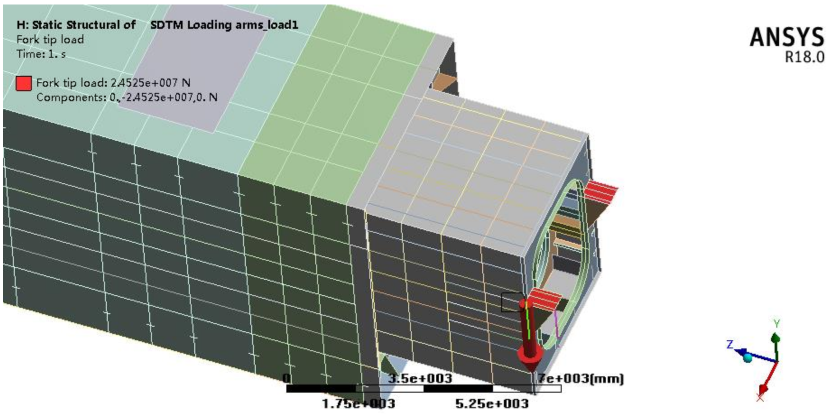

Fig. 11 The Load on the Fork Structure

The Ballast Tank Load: The ballast tank load is applied to the inner wall of the ballast tank in the form of hydrostatic pressure as shown in Figure 12. The pressure acting on the bottom is 0.1374 MPa, and the total load acting on the bottom is $F_{Ballast\ Tank} = 20702kN$, namely, 2111.2t.

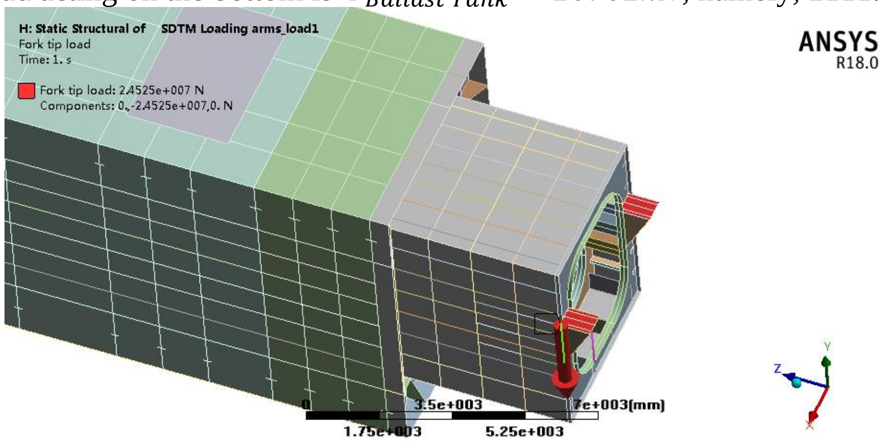

Fig. 12 The Load on the Ballast Tank Inner Wall

Buoyancy Tank Load: The buoyancy tank load is calculated through the moment balance of the other three loads. $F_{Ballast\ Tank}$, $F_{Buoyancy\ Tank}$ and F_{Fork} take moments from the fulcrum respectively. It is known that $F_{Ballast\ Tank} = 20702$kN, the distance from the action point of the ballast tank load to the fulcrum is $L_{Ballast\ Tank} = 29500$mm, F_{Fork}=24525kN, the distance from the action point of the load on the fork structure to the fulcrum L_{Fork}=41500mm, and the distance from the action point of the buoyancy tank load to the fulcrum $L_{Buoyancy\ Tank} =$ 29500mm=$L_{Ballast\ Tank}$. It is obtained $F_{Buoyancy\ Tank} = 13497$kN through moment balance calculation. This value is only 1.2% different from the original reported value of 13337kN. It shows that the error of the model is small as shown in Figure 13.

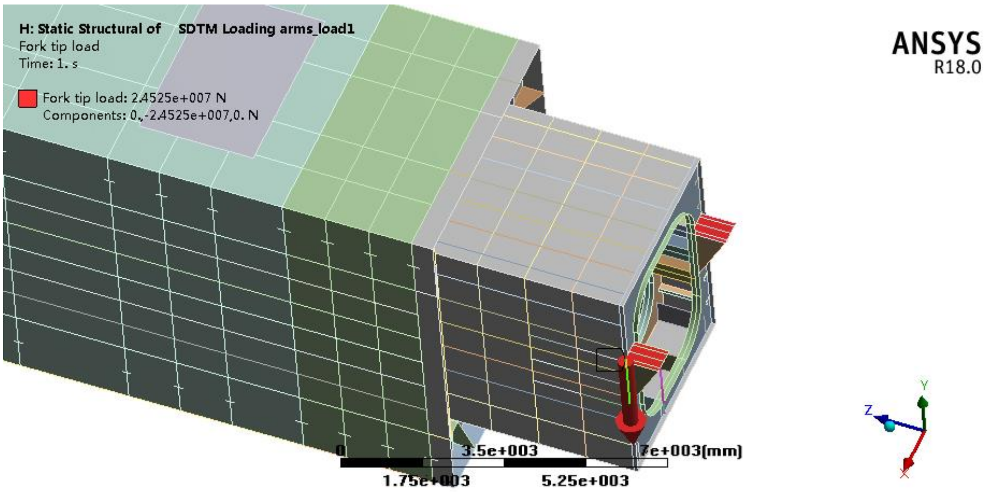

Fig. 13 The Load of the Buoyancy Tank

Setting of Constraints: The entire model only constrains the position of the shaft hole of the support frame and it shall rotate around the axis, which means that the model must meet the moment balance. In the internal structure of the lifting arm, the connection between the main arm and the telescopic arm is achieved through four rigid beams. The rigid beams are connected to the main arm and the telescopic arm using binding constraints respectively. The structure is as shown in Figure 14.

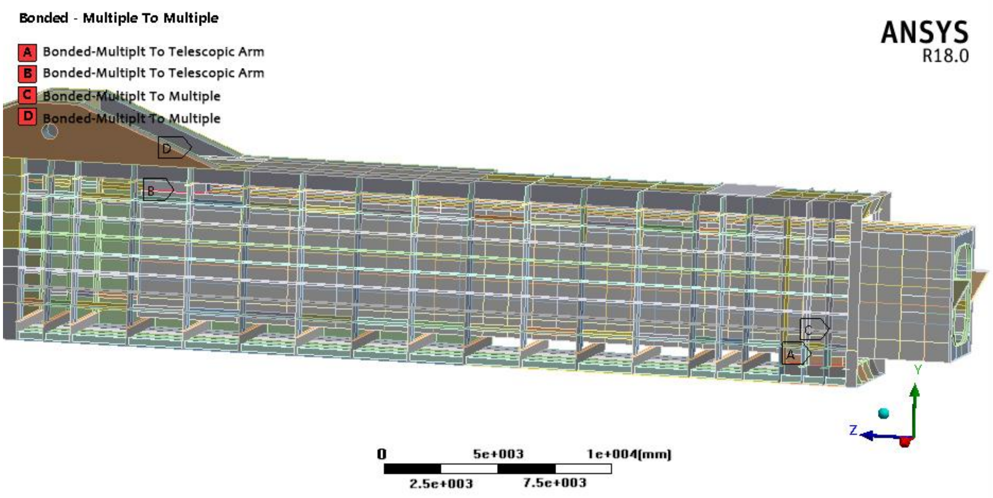

Fig. 14 The Connection Structure Between Main Arm and Telescopic Arm

3.2.2 The Loading Mode of the Experimental Model

In the design of the experimental model, the structure of the lifting arm is simplified and a servo electric cylinder is used to replace the dynamic actions of the ballast tank and buoyancy tank. There are two external loads on the lifting arm experimental model, namely the pressure on the fork structure and the lifting force of the electric cylinder, which is as shown in Figure 15.

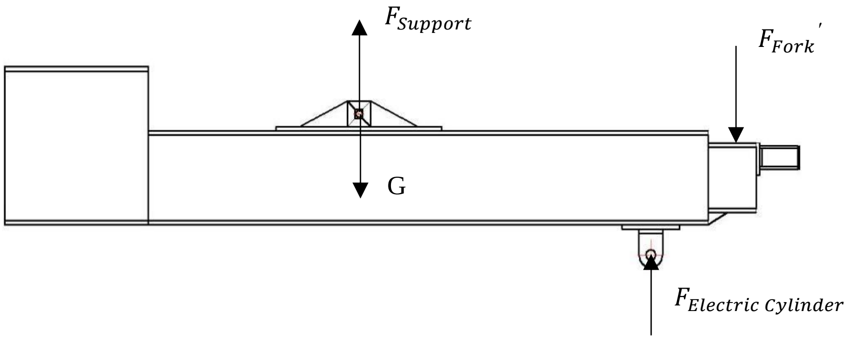

Fig. 15 The Force Diagram of the Lifting Arm Experimental Model

According to the similarity criterion of decommissioning equipment, $C_F = \dfrac{5\times10^5}{3}$ and $L_{Buoyancy\ Tank}{}' = 590\text{mm} = L_{Ballast\ Tank}{}'$, it can be calculated that $F_{Fork}{}'$=147.15N and $F_{Electric\ Cylinder}$=205.19N.

4. Simulation Analysis and Discussion

4.1. Simulation of the Lifting Arm Prototype

Establish the finite element model of the lifting arm in the software as shown in Figure 8. The material characteristics of the lifting arm is as shown in Table 1.

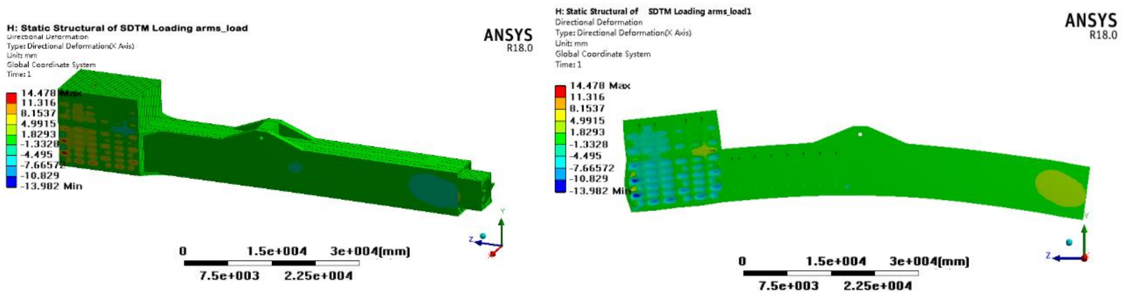

Fig. 16 Displacement Nephogram

It can be seen from the displacement nephogram results that the maximum displacement of the entire structure is 14.478mm, which occurs at the ballast tank and the contact point between the telescopic arm and the main arm. The main reason is that the ballast tank is filled with ballast water and the bottom bears a great force, and the thickness of the ballast tank needs to be adjusted. the contact point between the telescopic arm and the main arm is subject to a great force, so several reinforcing ribs are required. The overall structure meets the design requirements. From the displacement nephogram in Figure 16, it can be seen that the entire structure reaches moment balance about the center of rotation.

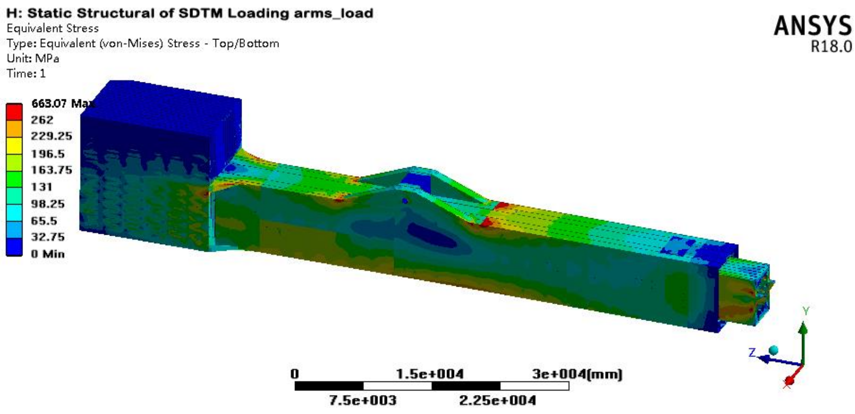

Fig. 17 Mises Stress of Lifting Arm

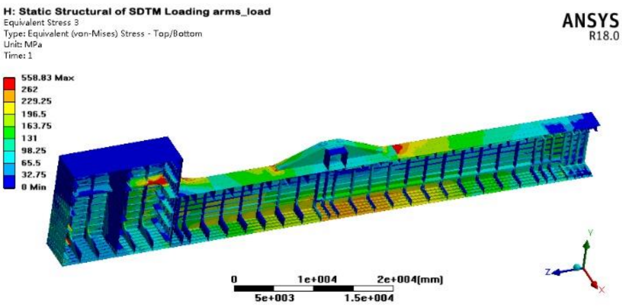

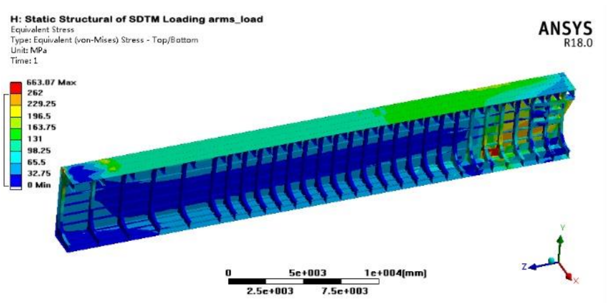

Fig. 18 Mises Stress of Main Arm **Fig. 19** Mises Stress of Telescopic Arm

According to the design requirements, the maximum allowable Mises stress of the lifting arm structure is 262MPa, and the maximum allowable shear stress is 151MPa.

It can be seen from the stress nephogram that only the equivalent stress at the position where the telescopic arm is connected to the rigid connecting beam exceeds the yield stress, all the rest parts of telescopic arm all meet the strength requirements. There are three parts of the main arm where the equivalent stress exceeds the allowable stress, which are the large transverse ribbed slab in the middle of the ballast tank where the ballast tank is connected to the main arm, the ribbed slab connecting the main arm and the ballast tank, and the connection between the support frame and the upper edge plate of the main arm. parts, and the strength of other parts meets the requirements.

4.2. Simulation of the Experimental Model of the Lifting Arm

The results of the simulation analysis is as shown in Figure 20. It can be seen from the displacement nephogram that the maximum displacement of the experimental model is 3.68mm which is within the reasonable range. The maximum displacement occurs at the tip of the fork structure contacting with the object to be lifted. It provides theoretic reference for manufacturing of the physical equipment and special treatment can be taken at critical positions.

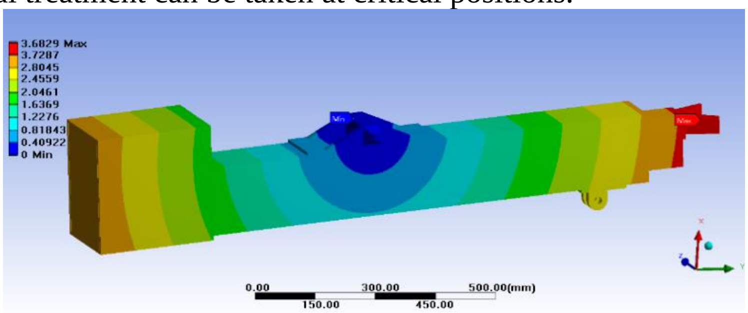

Fig. 20 Displacement Nephogram

5. Conclusion

In this article, a physical model of the lifting arm is established, and the positions where the maximum displacement occurs are obtained through finite element analysis. It is found that the bottom of the ballast tank is under great stress and needs to be thicker, the contact position between the telescopic arm and the main arm is under greater stress and needs to be strengthened with ribs, and the other parts meet the strength design requirements. Based on the principle of similitude, the lifting arm experimental model is designed and the relevant parameters are obtained. It is proved by finite element analysis that the designed experimental model meets the experimental requirements, which provides a theoretical basis for subsequent research.

References

[1] WANG I, DOWELL E H. Structural Dynamics Model of Multisegmented Folding Wings: Theory and Experiment [J]. Journal of aircraft, 2011, 48(6).

[2] Yuan Yongxin, Jiang Jiashang. A Non-overflow Model Correction Method Using Incomplete Modal Test Data [J]. Journal of Vibration and Shock, 2008, (07): 1-3+20+182.

[3] Chi Shichun, Lin Shaoshu. Validation of Similitude Laws for Structural Dynamic Model Test. World Earthquake Engineering, 2004, (04): 11-20.

[4] Liu Zeyu, Zhu Qiuchen. Similarity Analysis of Ship Lifting Machinery Model Test. Proceedings of the 2016 Academic Conference of the Testing Technology Group of the Ship Mechanics Academic Committee, Wuhan, Hubei, China, F, 2016 [C].

[5] LI D. Similarity theory which used in knuckle-joint press design; proceedings of the Proceedings of 2011 International Conference on Electronic & Mechanical Engineering and Information Technology, F 12-14 Aug. 2011, 2011 [C].

[6] Lan Huiqing, Ru Jixing, Zhang Ping. Research on Mechanical Characteristics of Cable-stayed Tube Bridges Based on the Theory of Similitude[J]. Petro-Chemical Equipment, 2013, 42(06): 1-5.

[7] LING LI, ANJIANG C, et al. Design of Heavy-load Beam Test Model Based on the Theory of Similitude. Proceedings of the Chinese Vibration Engineering Society; Chinese Society of Mechanics; Chinese Aeronautical Society; Chinese Mechanical Engineering Society; Chinese Astronautical Society, F, 2015 [C].

[8] Wang Zhenyu, Wang Tieshan, Song Li. Development and Application of 1:5 Scale Test Bench for Automobile Brake Linings [J]. Machinery Design and Manufacture, 2013, (02): 101-3.

[9] Song Rengqun. Similitude Principle of Clamp Bucket Strength, Stiffness and Stability and Similitude Conditions of Model Tests [J]. Journal of Wuhan University of Water Transportation Engineering, 1985, (01): 79-90.